

# A Partial-Multi-Conversion Single-Slope ADC with Response-Linearized RDAC

Akira Matsuzawa, Abdel Martinez Alonso, Lilan Yu, Minhyuk Sung and Masaya Miyahara  
 Tech Idea Co., Ltd., 1-21-5-1, Shukugawara, Tamaku, Kawasaki, 214-0021, Japan.  
 E-mail: [matsu@techidea.co.jp](mailto:matsu@techidea.co.jp), TEL: +81-44-385-2855

**ABSTRACT** This paper proposes a Single-Slope column ADC (SSADC) for CMOS Image Sensors (CIS). The response-linearized DAC using digital step pulse injection can realize a fast and accurate ramp wave without increase of power dissipation ( $P_d$ ). Low  $P_d$  of 0.9  $\mu$ W for a comparator is achieved with a resistive DAC (RDAC). The multi-conversion method is applied only for weak signal of less than 30 mV without significant increase in the conversion time,  $T_c$ . As a result, a 12bit SSADC attains a low noise of 32.5  $\mu$ V and a low  $P_d$  of 34  $\mu$ W while using 8 conversions at the  $T_c$  of 4  $\mu$ s. A high dynamic range of 90 dB and a high Schreier FoM<sub>S</sub> (DR) of 183 dB are attained with small size of 3.2  $\mu$ m x 556  $\mu$ m in 65 nm CMOS.

**KEYWORDS:** ADC, DAC, LOW NOISE, LOW POWER, CMOS, SENSOR, IMAGE SENSOR, COLUMN ADC, FOM.

## I. Introduction

A SSADC is a major column-ADC architecture used in CIS owing to its extremely short pitch and small area and channel mismatch. It however, continuously receives the demand for low noise operation [1]. On the other hand, it is exceedingly difficult to reduce the noise of the SSADC caused by the comparator. Fig. 1 shows a simplified comparator circuit for the SSADC.

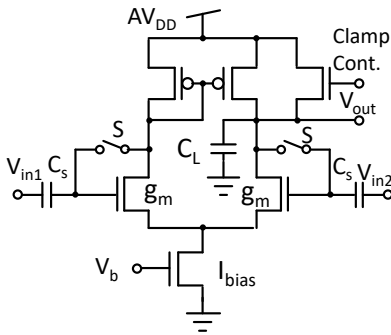


Fig. 1 Comparator circuit for the SSADC.

We have deduced the following noise equation at Correlated Double Sampling (CDS) operation [2].

$$\overline{v_{nc}} = \sqrt{8\sqrt{2}kT\gamma n_e} \left( \frac{V_{FS}}{2g_m V_{CL} C_L T_c} \right)^{0.25} \quad (1)$$

where, k: Boltzmann constant, T: temperature,  $\gamma$ : noise factor,  $n_e$ : effective number of transistors,  $V_{FS}$ : full scale ramp voltage,  $g_m$ : transconductance,  $V_{CL}$ : clamp voltage,

$C_L$ : load capacitance,  $T_c$ : conversion time. Fig. 2 shows our estimated noise by (1) is well matched with the simulation and the comparator noise can't be reduced easily mainly due to the power of 0.25 affecting the parameters in (1). Thus, the lowest noise is about 120  $\mu$ V at  $T_c$  of 1 $\mu$ s. Also increase of analog gain by reducing slope rate of the reference voltage is not efficient to reduce the noise. Noise voltage is about 2/3 if  $T_c$  is 16 times longer.

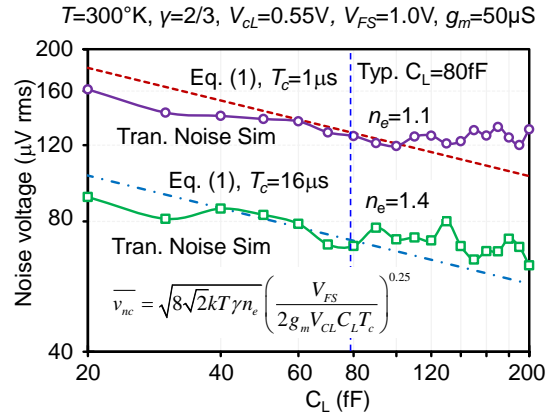


Fig. 2 Noise voltage vs. load capacitance.

The Shreier's FoM is based on physics for energy vs. noise. We estimated power dissipation vs noise voltage by using FoM<sub>S</sub> in consideration of CDS effect that the operation time is 1.5  $T_c$  and the noise voltage is 1.4 times larger and those reduce the FoM<sub>S</sub> by 4.8 dB. Fig. 3 shows the estimated  $P_d$  vs. noise voltage for the world's top FoM<sub>S</sub> (SNR) of 185 dB and practical FoM<sub>S</sub> of 180 dB and 175 dB [3] at  $T_c$  of 4  $\mu$ s. The  $P_d$  is rapidly increases with reducing the noise voltage. The  $P_d$  of current SSADC [1] is about 8 times larger than the estimation with FoM<sub>S</sub> of 175 dB.

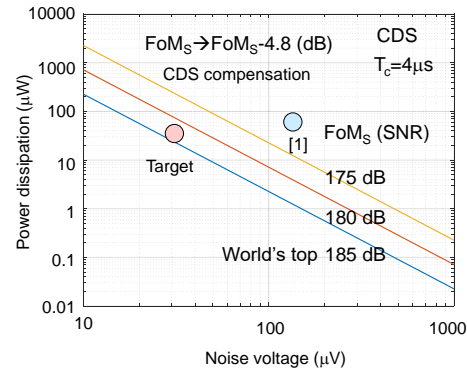


Fig. 3 Estimated power dissipation vs. noise voltage.

Our target (32  $\mu\text{V}$ , 35  $\mu\text{W}$ ) is almost on the line of the world's top FoMs and looks difficult to realize it. Another scenario for A/D conversion method is required.

## II. Partial-multi-conversion method

A multi-sampling method has been well known to reduce the readout noise in CIS [4]. The random noise voltage can be reduced by increasing the number of samplings,  $M$ . As a result,  $T_c$  is increased by increasing  $M$ . It limits the application to the moving picture. For example, noise voltage of 75  $\mu\text{V}$  was obtained by  $M$  of 5, however  $T_c$  is 27  $\mu\text{s}$  and the frame rate is only 7.2 frames/s [5].

Fig. 4 shows our proposed Partial-Multi-Conversion (PMC) method. Two DACs, one is a Local DAC (LDAC) for converting limited voltage range and the other is a Global DAC (GDAC) for full voltage range are used.

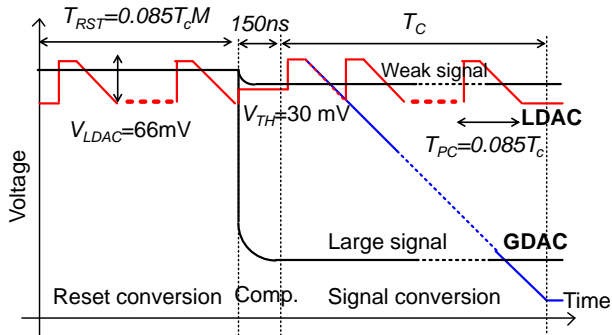


Fig. 4 Partial-Multi-Conversion (PMC) method.

The SSADC converts the reset signal  $M$  times with LDAC during reset-conversion within a limited range of about 66 mV. Next, the signal is compared to the threshold voltage,  $V_{TH}$  of 30 mV within about 200 ns in order to select the LDAC or the GDAC. The GDAC is selected to convert the full range of 1.0 V for large signal. The LDAC is selected to convert the weak signal  $M$  times within a partial range of about 66 mV. The threshold voltage should be determined by considering the shot noise. Fig. 5 shows the signal voltage, the shot noise of the photo-diode at the conversion gain of 30  $\mu\text{V}/e^-$ , and the ADC readout noise.

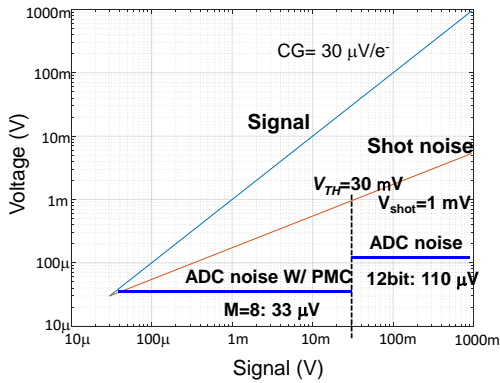


Fig. 5 Signal, shot noise, and ADC noise.

The shot noise at the threshold voltage of 30 mV is about 1 mV. The ADC noise is low enough compared to the shot noise and the SSADC has a sufficient voltage margin to tolerate the error voltage at the DAC switching point.

The proposed PMC method only requires extra conversion time during the reset conversion period and doesn't require it to the signal conversion period. However, the required reset time is only 3.0  $\mu\text{s}$  for  $T_c = 4.0 \mu\text{s}$  and  $M = 8$ . Furthermore, the proposed PMC method can reduce the pixel noise as well as the ADC noise. The noise power transfer function NTF is

$$NTF(\omega) = \left| 1 - e^{-j\omega T_{CDS}} \right|^2 \left| \frac{1 - e^{-j\omega M T_{PC}}}{1 - e^{-j\omega T_{PC}}} \right|^2 \quad (2)$$

where  $T_{CDS}$  is the period of CDS and  $T_{PC}$  is the period of the partial multi conversion. Therefore, the PMC can additionally suppress the high frequency noise components of the  $1/f$  noise, as shown in Fig. 6.

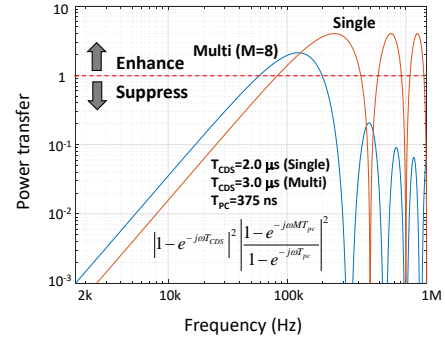


Fig. 6 Noise power transfer of the PMC.

## III. Response-linearized RDAC

A fast and accurate ramp signal generation is vitally required for the PMC. However, the nonlinearity of the response caused by RC delay deteriorates the accuracy of the ramp waveform. Conventionally, the reduction of output resistance or voltage buffer are used but this results in an increase of  $P_d$ . We have solved this issue by controlling the input data of the DAC. Fig. 7 shows the DAC including an RC circuit at the output terminal.

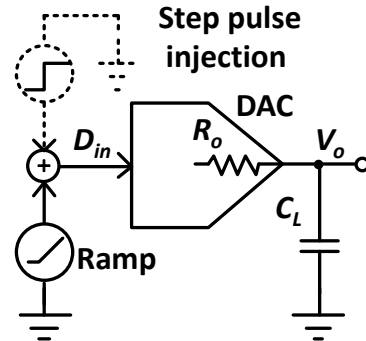


Fig. 7 DAC including an RC circuit at the output.

The output voltage  $V_o$  to the input ramp data is

$$V_o(t) = S_R \cdot t - S_R \cdot \tau \left(1 - e^{-\frac{t}{\tau}}\right) \quad (3)$$

where  $S_R$  is the slew-rate of the ramp signal and  $\tau$  is the time constant of  $R_o C_L$ . Fig. 8 shows the input and output waveforms of the conventional and the proposed DAC. The output voltage of the conventional DAC is delayed and distorted. The second term in (3) expresses the error and it can be cancelled by injecting the digital step-pulse to the input of the DAC.

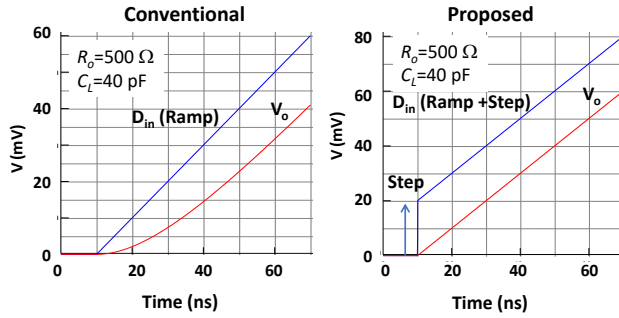


Fig. 8 Input and output waveforms of the conventional and the proposed DAC.

The delay and distortion of the proposed DAC are clearly canceled without any increase in  $P_d$ , if the digital step pulse is injected to the DAC. Fig. 9 shows the  $P_d$  is 8 times lower while achieving the same INL for the LDAC.

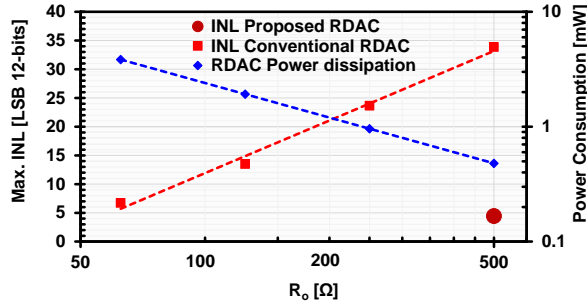


Fig. 9 Linearity and power dissipation vs.  $R_o$  in DAC.

The digital calibration can find the optimal value for the injection step within a short time of 4  $\mu$ s to linearize the DAC response.

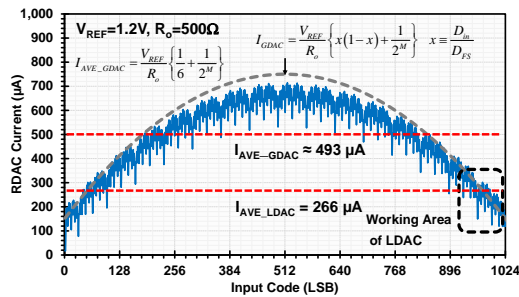


Fig.10 Currents of the GDAC and the LDAC.

Furthermore, we used an RDAC instead of a conventional current DAC (IDAC) to reduce the  $P_d$ . Fig. 10 shows the power supply current of the 10bit RDAC vs. input code. The average currents of GDAC and LDAC at  $R_o$  of 500  $\Omega$  are only 493  $\mu$ A and 266  $\mu$ A. Those are 1/4 and 1/8 of the conventional IDAC. Two RDACs consume only 0.9 mW in total and 0.9  $\mu$ W for each comparator.

#### IV. SSADC and test chip design

Fig.11 shows the SSADC and Fig. 12 shows the clocks for the Time to Digital Converter (TDC). The comparator uses a conventional cascode amplifier with DAC selection switch. A 4bit TDC uses four dual-edge Gray-code clocks to reduce the  $P_d$ . The average  $P_d$  of the ADC is 34  $\mu$ W.

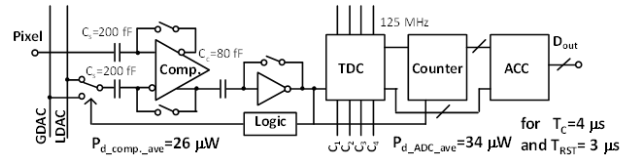


Fig. 11 Block diagram of the SSADC.

#### Effective clock freq. =2 GHz for $T_c=2 \mu$ s

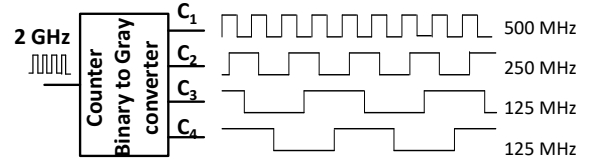


Fig. 12 Dual edge Gray-coded clocks for the TDC.

The size of the ADC is 3.2  $\mu$ m x 556  $\mu$ m, and the test chip integrates 960 ADCs in 65nm CMOS, as shown in Fig. 13.

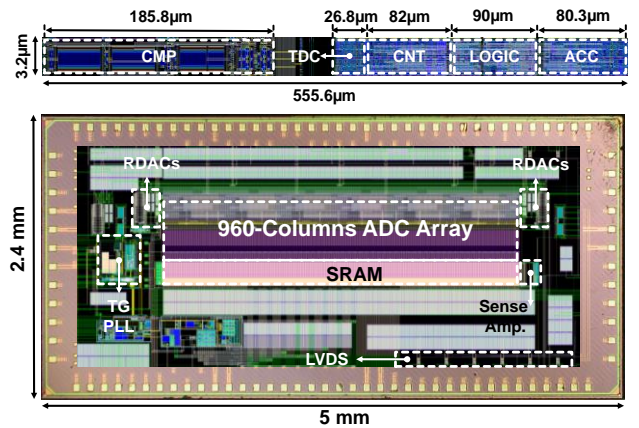


Fig.13 Layout of the SSADC and photo of the test chip.

#### V. Experimental results

Fig. 14 shows the measured noise voltages after CDS for  $T_c=2, 3, 4 \mu$ s and  $M=1, 2, 4, 8$ . At  $T_c=4 \mu$ s, the noise voltage with  $M=1$  is about 120  $\mu$ V and almost same as the

simulated value. The noise can be reduced to 32  $\mu\text{V}$  when  $M=8$ . At  $T_c=2 \mu\text{s}$ , the noise voltage with  $M=1$  is about 300  $\mu\text{V}$ , which is three times larger than the simulated value. However, the multi-conversion still works and a noise voltage of 70  $\mu\text{V}$  is obtained when  $M=8$ .

Fig. 15 shows the output codes of the ADC around the  $V_{TH}$  crossing point for the nearest and the farthest ADC from the DAC. The worst-case gap voltage is 230  $\mu\text{V}$  and well below the shot noise of 1 mV. Measured DNL and channel mismatch are only 0.08 LSB both. Power dissipation of ADC and DAC with CDS at  $T_c=4 \mu\text{s}$  and  $M=8$  is 34  $\mu\text{W}$  and 0.9  $\mu\text{W}$  for one column. The dynamic range is 90 dB and the Schreier FoM<sub>S</sub> is 183 dB (DR) and 174 dB (SNR). This performance is competitive compared to CT  $\Delta\Sigma$  ADCs for sensors [6] while the area the SSADC is 150 times smaller. Table 1 summarizes the performance.

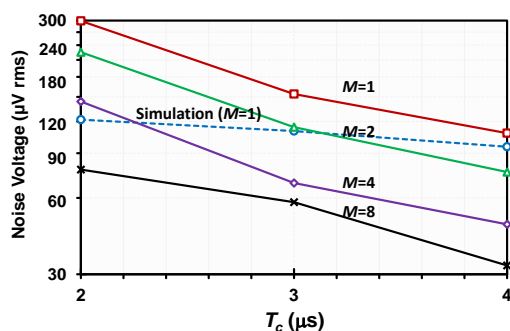


Fig. 14 The measured noise voltages vs.  $T_c$  after CDS for  $T_c=2, 3, 4 \mu\text{s}$  and  $M=1, 2, 4, 8$ .

## VI. Conclusion

The response-linearized RDAC using digital step pulse injection can realize the fast and accurate ramp wave. Small  $P_d$  of 0.9  $\mu\text{W}$  in the DAC for a comparator is achieved.

Table 1. Performance summary and comparison.

	This work			[1]	[5]	[6]
ADC architecture	SS			SS in CIS	SS in CIS	CT $\Delta\Sigma$
Resolution (bit)	12			12	11	
Full scale voltage and LSB voltage:	1.0 V(Full), 244 $\mu\text{V}$ (LSB)			923 mV, 225 $\mu\text{V}$		
INL: p-p (LSB) and DNL: $\sigma$ (LSB)	-2.4/2.2 (INL), 0.08 (DNL)					
Channel mismatch voltage: $\sigma$ (LSB)	0.08					
Worst-case voltage gap at $V_{TH}$ for $T_c=4 \mu\text{s}$ : p-p ( $\mu\text{V}$ )	230					
$P_d$ of GDAC+LDAC and $P_d$ for one comparator	0.9 mW, 0.9 $\mu\text{W}/\text{comp.}$			32 $\mu\text{W}/\text{comp.}$		
Period of reset conversion for $T_c=4 \mu\text{s}$ and $M=8$ ( $\mu\text{s}$ )	3.0					
$P_d$ ( $\mu\text{W}$ ) and $E_d$ (pJ/conv.) of ADC w/ CDS for $T_c=4 \mu\text{s}$ and $M=8$	34 ( $P_d$ ), 237 ( $E_d$ )			48.8, 341 estim.		55, 1375
Area of ADC ( $\mu\text{m}^2$ )	3.2 x 556 = 1,778					270,000
Conversion time $T_c$ : ( $\mu\text{s}$ )	2.0	3.0	4.0	1.53	27.6	25
$V_n$ ( $\mu\text{V}$ ) rms at $M=1$	299.0	154.0	108.0	140.0		
$V_n$ ( $\mu\text{V}$ ) rms at $M=2$	225.0	114.0	75.9			
$V_n$ ( $\mu\text{V}$ ) rms at $M=4$	143.9	68.7	47.2		73 (M=5)	
$V_n$ ( $\mu\text{V}$ ) rms at $M=8$	77.6	57.7	32.5			
Dynamic range and SNR for $T_c=4 \mu\text{s}$ and $M=8$ (dB)	90 (DR), 81 (SNR)			76.3 (DR)		93 (DR)
FoMs(DR) and FoMs(SNR) w/ CDS for $T_c=4 \mu\text{s}$ and $M=8$ (dB)	183 (DR), 174 (SNR)			167 (DR) estim.		179 (DR)

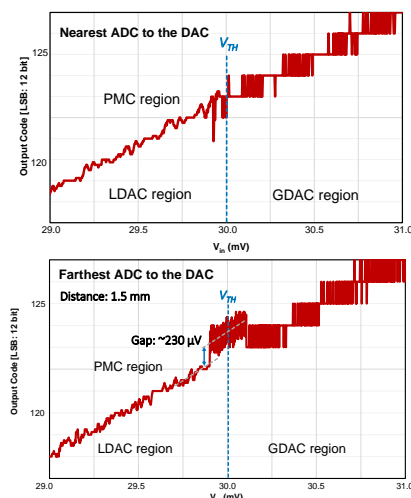


Fig. 15 Measured ADC outputs around  $V_{TH}$ . (Nearest and furthest from the DAC.)

The partial multi-conversion method with a 12bit SSADC attained a low noise of 32.5  $\mu\text{V}$  and a low  $P_d$  of 34  $\mu\text{W}$  at  $T_c=4 \mu\text{s}$  and  $M=8$  with CDS. A high dynamic range of 90 dB and a high Schreier FoM<sub>S</sub> (DR) of 183 dB are attained.

## Acknowledgement

This paper is based on results obtained from a project, JPNP18004, subsidized by the New Energy and Industrial Technology Development Organization (NEDO).

## References

- [1] Y. Oike et al., IEEE JSSC, pp. 958-992, April. 2017.
- [2] A. Matsuzawa et al., IISW, pp. 324-327, May. 2017.
- [3] B. Murmann, ADC Performance survey 1997-2021. <http://web.stanford.edu/~murmann/adcsurvey.html>.
- [4] S. Kawahito et al., IISW, June 2009.
- [5] S-F. Yeh et al., IEEE JSSC, pp. 527-537, Feb. 2018.
- [6] M-H. Jang et al., IEEE Symp. on VLSI circuits 2017.